Numerical simulation of cubic-quartic optical soliton perturbation with Lakshmanan-Porsezian-Daniel model by Laplace-Adomian decomposition

O. GONZÁLEZ – GAXIOLA[1], ANJAN BISWAS[2,3,4,5,6,*], YAKUP YILDIRIM[7], HASHIM M. ALSHEHRI[3]
[1]*Applied Mathematics and Systems Department, Universidad Autónoma Metropolitana-Cuajimalpa, Vasco de Quiroga 4871, 05348 Mexico City, Mexico*
[2]*Department of Mathematics and Physics, Grambling State University, Grambling, LA—71245, USA*
[3]*Mathematical Modeling and Applied Computation (MMAC) Research Group, Department of Mathematics, King Abdulaziz University, Jeddah–21589, Saudi Arabia*
[4]*Department of Applied Sciences, Cross-Border Faculty, Dunarea de Jos University of Galati, 111 Domneasca Street, Galati-800201, Romania*
[5]*Department of Mathematics and Applied Mathematics, Sefako Makgatho Health Sciences University, Medunsa–0204, Pretoria, South Africa*
[6]*Department of Applied Mathematics, National Research Nuclear University, 31 Kashirskoe Hwy, Moscow–115409, Russian Federation*
[7]*Department of Computer Engineering, Biruni University, 34010 Istanbul, Turkey*

This paper studies cubic-quartic optical soliton dynamics numerically. The model is governed by Lakshmanan-Porsezian-Daniel equation that is addressed by the application of Laplace-Adomian decomposition scheme. Bright and dark soliton solutions are studied and the appealing error measures are also displayed.

(Received December 31, 2021; accepted August 10, 2022)

Keywords: Nonlinear Schrödinger equation, Lakshmanan-Porsezian-Daniel model, Solitons, Laplace transforms, Adomian decomposition method

1. Introduction

One of the most viable models to address soliton propelling dynamics through optical fibers and/or metamaterials is the Lakshmanan-Porsezian-Daniel (LPD) equation [1, 2, 3]. This model was studied earlier by several authors where chromatic dispersion (CD) was the source of dispersive effects. Later, this model was modified, when CD maintains a low count, to accommodate third-order dispersion (3OD) and fourth-order dispersion (4OD) effects which are collectively termed as cubic-quartic (CQ) effect and hence the concept of CQ solitons. One immediate question that arises is the effect of soliton radiation and the slowdown of such solitons. These effects are ignored for the LPD model so that the focus is on the core soliton region.

The focus of the paper is to address this LPD model numerically to gain a visual perspective to the soliton dynamics in one-dimensional setting. The adopted numerical scheme is the combination of the pre-existing Laplace transform and the well-known Adomian decomposition scheme to formulate the combined Laplace-Adomian decomposition method (LADM). This scheme has been successfully applied to retrieve solitons, Gaussons and highly dispersive solitons in optical fibers [4, 5, 6, 7, 8, 9]. Today, the same integration tool will be applied to numerically study bright and dark solitons that has emerged from the model and has been reported [1, 2]. The perturbed bright and dark CQ soliton solutions have already been recovered analytically by the sine-Gordon equation approach, the method of undetermined coefficients as well as the semi-inverse variational principle [1, 2, 3]. The numerical scheme is detailed and the respective surface plots for bright as well as dark CQ solitons are exhibited. The error measures are also tabulated, and these are truly eye appealing. The details are depicted in the rest of the paper.

1.1. Description of the Lakshmanan-Porsezian-Daniel model

In the presence of perturbation terms, the Lakshmanan-Porsezian-Daniel (LPD) equation is written as [1]:

$$iq_t + iaq_{xxx} + bq_{xxxx} + c|q|^2q - \alpha(q_x)^2q^*$$
$$-\beta|q_x|^2q - \gamma|q|^2q_{xx} - \lambda q^2q^*_{xx} - \delta|q|^4q$$
$$-i[\zeta(|q|^{2m}q)_x + \mu(|q|^{2m})_xq + \rho|q|^{2m}q_x] = 0, \quad (1)$$

where $q(x,t)$ stands for the complex-valued wave profile, where x and t are respectively spatial and temporal variables. The first term represents linear temporal evolution and $i=\sqrt{-1}$. a and b denote coefficients of 3OD and 4OD, respectively. Moreover, the perturbation terms come from self-steepening effect that is stood for by ζ. Lastly, the coefficients of μ and ρ give the effect of nonlinear dispersions.

2. Bright and dark solitons for the governing model (1) for the case $m=1$

The bright solitons to the perturbed LPD equation (1) considering $m=1$ were recently established for the first time, using the method of undetermined coefficients by the authors in [1] and these are given by means of

$$q(x,t)=A_1\mathrm{sech}[B_1(x-\nu t)]$$
$$\times\exp\{i(-\kappa x+\omega t+\theta)\}, \tag{2}$$

where the soliton amplitude A_1 is given in terms of the model parameters by

$$A_1=\sqrt{\frac{4bB^2(3\kappa^2+5B^2)}{\Gamma_1-(\Gamma_2+\Gamma_3)B^2}}, \tag{3}$$

and the width B_1 is given in terms of the model parameters by

$$B_1=\sqrt{\frac{-(7\Gamma_2+2\Gamma_3\pm5\Gamma_B)\Gamma_1+3[40b\delta+(\Gamma_2+\Gamma_3)(\Gamma_2+3\Gamma_3\pm\Gamma_B)]\kappa^2}{2[100b\delta-(\Gamma_2-4\Gamma_3)(\Gamma_2+\Gamma_3)]}}, \tag{4}$$

where, to simplify the notation, we have

$$\Gamma_1=c+\kappa^2(2\lambda-\beta),\Gamma_2=\alpha+\beta,$$
$$\Gamma_3=\gamma+\lambda,\ \Gamma_B=\sqrt{96b\delta+(\Gamma_2+2\Gamma_3)^2}, \tag{5}$$

provided

$$[100b\delta-(\Gamma_2-4\Gamma_3)(\Gamma_2+\Gamma_3)][(7\Gamma_2+2\Gamma_3\pm5\Gamma_B)\Gamma_1$$
$$+3[40b\delta+(\Gamma_2+\Gamma_3)(\Gamma_2+3\Gamma_3\pm\Gamma_B)]\kappa^2]<0, \tag{6}$$

and

$$96b\delta+(\Gamma_2+2\Gamma_3)^2\geq0. \tag{7}$$

The dark solitons to the perturbed LPD equation (1) considering $m=1$ were also established in [1] and these are given by means of

$$q(x,t)=A_2\tanh[B_2(x-\nu t)]$$
$$\times\exp\{i(-\kappa x+\omega t+\theta)\}, \tag{8}$$

where the soliton amplitude A_1 is given in terms of the model parameters by

$$A_2=\sqrt{\frac{4bB^2(10B^2-3\kappa^2)}{\Gamma_1+2(\Gamma_2+\Gamma_3)B^2}}, \tag{9}$$

and the width B_1 is given in terms of the model parameters by

$$B_2=\sqrt{\frac{\Gamma_1(7\Gamma_2+2\Gamma_3)+3\kappa^2[40b\delta+(\Gamma_2+\Gamma_3)(\Gamma_2+2\Gamma_3]\pm\Gamma_D}{4[100b\delta-(\Gamma_2-4\Gamma_3)(\Gamma_2+\Gamma_3)]}}, \tag{10}$$

where Γ_1, Γ_2 and Γ_3 are the same as in (5) and

$$\Gamma_D=[5\Gamma_1+3\kappa^2(\Gamma_2+\Gamma_3)]\sqrt{96b\delta+(\Gamma_2+2\Gamma_3)^2}. \tag{11}$$

Subject to the same restriction given in Eq. (7) and in addition with the constraint

$$[100b\delta-(\Gamma_2-4\Gamma_3)(\Gamma_2+\Gamma_3)][\Gamma_1(7\Gamma_2+2\Gamma_3)$$
$$+3\kappa^2[40b\delta+(\Gamma_2+\Gamma_3)(\Gamma_2+2\Gamma_3]\pm\Gamma_D]>0. \tag{12}$$

3. The Laplace transform combined with Adomian decomposition method

In this section we will briefly develop the well-known Adomian decomposition method and its improvement resulting from combining the method with the Laplace transform [10, 11]. The development is focused on achieving both bright and dark solitons for the LPD equation model (1) for the case $m=1$.

The LPD equation given in (1) in an operator form is

$$D_tq(x,t)+Rq(x,t)+Nq(x,t)=0, \tag{13}$$

with initial condition

$$q(x,0)=f(x), \tag{14}$$

where $D_tq=iq_t$ is the usual time derivation operator, Rq is a linear differential operator, which in our case turns out to be

$$Rq(x,t)=iaq_{xxx}+bq_{xxxx}, \tag{15}$$

while Nq is a nonlinear operator, which acts as a

$$Nq(x,t)=c|q|^2q-\alpha(q_x)^2q^*-\beta|q_x|^2q$$
$$-\gamma|q|^2q_{xx}-\lambda q^2q_{xx}^*-\delta|q|^4q$$
$$-i[\zeta(|q|^2q)_x+\mu(|q|^2)_xq+\rho|q|^2q_x]. \tag{16}$$

According to the standard Adomian decomposition method, the solution q can be expanded in an infinite series as follows:

$$q(x,t)=\sum_{n=0}^{\infty} q_n(x,t), \tag{17}$$

and the nonlinear term series

$$Nq(x,t)=\sum_{n=0}^{\infty} A_n(q_0,\cdots,q_n), \tag{18}$$

where A_n are the Adomian polynomials.

In the case of the nonlinear operator given in Eq. (16), we can decompose it as

$$Nq(x,t)=\sum_{j=1}^{9} N_j q(x,t), \tag{19}$$

where:

$$N_1 q = c|q|^2 q, N_2 q = \alpha(q_x)^2 q^*,$$

$$N_3 q = \beta|q_x|^2 q, N_4 q = \gamma|q|^2 q_{xx},$$

$$N_5 q = \lambda q^2 q_{xx}^*, N_6 q = \delta|q|^4 q, N_7 q = i\zeta(|q|^2 q)_x,$$

$$N_8 q = i\mu(|q|^2)_x q,\ N_9 q = i\rho|q|^2 q_x. \tag{20}$$

Then each of the nonlinear terms $N_j q,\ 1\le j\le 9$, can be decomposed into infinite series of Adomian polynomials given by:

$$N_1 q = c|q|^2 q = \sum_{n=0}^{\infty} A_n^{(1)}(q_0,q_1,\cdots,q_n), \tag{21}$$

$$N_2 q = \alpha(q_x)^2 q^* = \sum_{n=0}^{\infty} A_n^{(2)}(q_0,q_1,\cdots,q_n), \tag{22}$$

$$N_3 q = \beta|q_x|^2 q = \sum_{n=0}^{\infty} A_n^{(3)}(q_0,q_1,\cdots,q_n), \tag{23}$$

$$N_4 q = \gamma|q|^2 q_{xx} = \sum_{n=0}^{\infty} A_n^{(4)}(q_0,q_1,\cdots,q_n), \tag{24}$$

$$N_5 q = \lambda q^2 q_{xx}^* = \sum_{n=0}^{\infty} A_n^{(5)}(q_0,q_1,\cdots,q_n), \tag{25}$$

$$N_6 q = \delta|q|^4 q = \sum_{n=0}^{\infty} A_n^{(6)}(q_0,q_1,\cdots,q_n), \tag{26}$$

$$N_7 q = i\zeta(|q|^2 q)_x = \sum_{n=0}^{\infty} A_n^{(7)}(q_0,q_1,\cdots,q_n), \tag{27}$$

$$N_8 q = i\mu(|q|^2)_x q = \sum_{n=0}^{\infty} A_n^{(8)}(q_0,q_1,\cdots,q_n), \tag{28}$$

$$N_9 q = i\rho|q|^2 q_x = \sum_{n=0}^{\infty} A_n^{(9)}(q_0,q_1,\cdots,q_n). \tag{29}$$

In the expressions (21)-(29) above, the $A_n^{(j)}$ are the Adomian polynomials corresponding to the nonlinear terms N_j. These can be calculated by the formulas shown in [12], that is,

$$A_n^{(j)}(q_0,q_1,\dots,q_n)=$$

$$\begin{cases} N_j(q_0), & n=0 \\ \frac{1}{n}\sum_{k=0}^{n-1}(k+1)q_{k+1}\frac{\partial}{\partial q_0}A_{n-1-k}^{(j)}, & n=1,2,3,\dots \end{cases} \tag{30}$$

From now on $\mathcal{L}$ will denote the Laplace transform and $\mathcal{L}^{-1}$ its inverse operator. Then applied $\mathcal{L}$ on both sides of Eq. (13) we have

$$\mathcal{L}\{D_t q(x,t)+Rq(x,t)+Nq(x,t)\}=0, \tag{31}$$

and using initial condition, which will be derived from the initials profiles of the solitons f, we obtian

$$\mathcal{L}\{q(x,t)\}=\frac{1}{s}f(x)$$

$$-\frac{1}{s}(\mathcal{L}\{Rq(x,t)\}+\mathcal{L}\{Nq(x,t)\}). \tag{32}$$

Substituting Eqs. (17)–(18) into Eq. (32), it gives

$$\mathcal{L}\{\sum_{n=0}^{\infty} q_n(x,t)\}=\frac{1}{s}f(x)$$

$$-\frac{1}{s}(\mathcal{L}\{R(\sum_{n=0}^{\infty} q_n(x,t))\}$$

$$+\mathcal{L}\{\sum_{n=0}^{\infty} A_n(q_0,\dots,q_n)\}). \tag{33}$$

Applying the linearity of Laplace transform in Eq. (33), we obtain

$$\sum_{n=0}^{\infty}\mathcal{L}\{q_n(x,t)\}=\frac{1}{s}f(x)$$

$$-\frac{1}{s}(\sum_{n=0}^{\infty}\mathcal{L}\{Rq_n(x,t)\}$$

$$+\sum_{n=0}^{\infty}\mathcal{L}\{A_n(q_0,\dots,q_n)\}). \tag{34}$$

then, considering the process of decomposition in the Adomian polynomials (19)-(29) we obtain

$$\sum_{n=0}^{\infty}\mathcal{L}\{q_n(x,t)\}=\frac{1}{s}f(x)$$

$$-\frac{1}{s}(\sum_{n=0}^{\infty}\mathcal{L}\{Rq_n(x,t)\}$$

$$+\sum_{j=1}^{9}[\sum_{n=0}^{\infty}\mathcal{L}\{A_n^{(j)}(q_0,\cdots,q_n)\}]). \tag{35}$$

Matching both sides of Eq. (33), we obtain the Laplace transform of each of the components of the solution, that is

$$\mathcal{L}\{q_0(x,t)\}=\frac{1}{s}f(x), \tag{36}$$

and for every $m\ge 1$, the recursive relations are given by

$$\mathcal{L}\{q_m(x,t)\}=-\frac{1}{s}(\mathcal{L}\{Rq_{m-1}(x,t)\}$$

$$+\sum_{j=1}^{9}\mathcal{L}\{A_{m-1}^{(j)}(q_0,\dots,q_{m-1})\}). \tag{37}$$

Finally, the components q_0, q_1, q_2, . . . , are then determined recursively by using inverse Laplace transform:

$$q_0(x,t) = f(x),$$

$$q_m(x,t) = -\mathcal{L}^{-1}(\frac{1}{s}\mathcal{L}\{Rq_{m-1}(x,t)\}$$

$$+\frac{1}{s}\sum_{j=1}^{9} \mathcal{L}\{A_{m-1}^{(j)}(q_0,\dots,q_{m-1})\}),\ m \geq 1, \quad (38)$$

where q_0 is referred to as the zero-th component. An $N-$components truncated series solution is thus obtained as

$$S_N = \sum_{i=0}^{N} q_i(x,t). \quad (39)$$

The series solution (39) can be used for numerical purposes. For further detail about the convergence of the proposed method, we refer [13].

In the next section, some numerical examples are given to illustrate the high accuracy and efficiency of the algorithm provided by the proposed method.

4. Test examples

In this section, some examples are provided to show the efficiency and accuracy of the suggested method to find soliton solutions of the LPD equation given by (1). The numerical simulation results are carried out by using the *Mathematica* software.

4.1. Bright highly dispersive optical soliton

We now consider the initial condition at $t = 0$ from Eq. (2):

$$f(x) = A_1\text{sech}(B_1x)\exp\{i(-\kappa x+\theta)\}. \quad (40)$$

We will carry out the simulation for the Cases 1, 2 and 3, respectively with the parameters given in Table 1. The results obtained are shown graphically in Figs. 1, 2 and 3. In addition, Tables 2, 3 and 4 show the absolute errors for various points in space-time.

Table 1. Coefficients of Eq. (1) to simulate bright solitons

a	b	c	α	β	γ	λ	δ	ζ	μ	ρ	N
0.32	0.30	1.02	2.26	1.22	1.04	0.71	0.14	1.14	0.93	1.11	14
1.23	2.04	1.79	2.08	1.10	2.54	2.62	0.44	0.08	4.50	2.37	14
0.50	1.80	0.75	4.27	8.02	3.22	0.65	3.06	3.04	2.56	1.45	15

Table 2. Absolute error in space-time for 14^{th} iteration of Case 1

(t,x)	-3.0	-2.0	-1.0	1.0	2.0	3.0
0.1	6.03×10^{-8}	4.15×10^{-8}	1.22×10^{-8}	1.29×10^{-8}	4.09×10^{-8}	6.29×10^{-8}
0.3	8.58×10^{-8}	6.22×10^{-8}	3.08×10^{-8}	2.92×10^{-8}	5.98×10^{-8}	7.98×10^{-8}
0.5	8.32×10^{-7}	4.42×10^{-7}	3.44×10^{-7}	3.95×10^{-7}	4.05×10^{-7}	8.84×10^{-7}

Table 3. Absolute error in space-time for 14^{th} iteration of Case 2

(t,x)	-3.0	-2.0	-1.0	1.0	2.0	3.0
0.1	7.88×10^{-8}	6.20×10^{-8}	4.38×10^{-8}	4.09×10^{-8}	6.38×10^{-8}	8.01×10^{-8}
0.3	9.29×10^{-8}	4.29×10^{-8}	4.88×10^{-8}	1.07×10^{-8}	4.13×10^{-8}	8.44×10^{-8}
0.5	9.31×10^{-7}	5.82×10^{-7}	2.23×10^{-7}	2.74×10^{-7}	4.95×10^{-7}	8.94×10^{-7}

Table 4. Absolute error in space-time for 15^{th} iteration of Case 3

(t,x)	-3.0	-2.0	-1.0	1.0	2.0	3.0
0.1	6.07×10^{-8}	5.71×10^{-8}	5.43×10^{-9}	4.77×10^{-9}	6.04×10^{-8}	7.01×10^{-8}
0.3	8.11×10^{-8}	7.29×10^{-8}	6.34×10^{-9}	6.56×10^{-9}	7.88×10^{-8}	8.08×10^{-8}
0.5	9.56×10^{-7}	8.02×10^{-7}	6.18×10^{-8}	6.31×10^{-8}	7.95×10^{-7}	9.88×10^{-7}

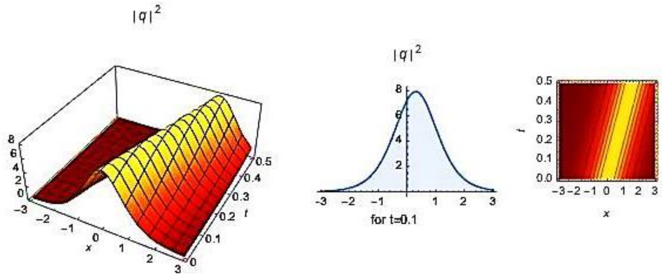

Fig. 1. 3D, 2D and density graphics for Case 1 (color online)

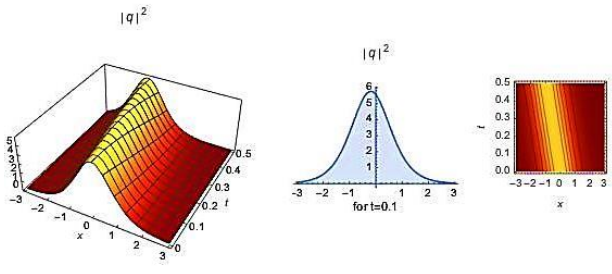

Fig. 2. 3D, 2D and density graphics for Case 2 (color online)

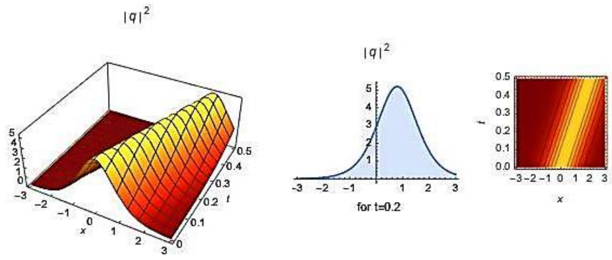

Fig. 3. 3D, 2D and density graphics for Case 3 (color online)

4.2. Dark highly dispersive optical soliton

We now consider the initial condition at $t = 0$ from Eq. (8):

$$f(x) = A_2 \tanh(B_2 x) \exp\{i(-\kappa x + \theta)\}. \quad (41)$$

We will carry out the simulation for the Cases 4, 5 and 6 respectively with the parameters given in Table 5. The results obtained are shown graphically in Figs. 4, 5 and 6. In addition, Tables 6, 7 and 8 show the absolute errors for various points in space-time.

Table 5. Coefficients of Eq. (1) to simulate dark solitons

	b	c	α	β	γ	λ	δ	ζ	μ	ρ	N
1.02	1.10	0.02	1.02	2.22	3.04	1.21	3.14	0.24	1.33	2.33	14
0.28	2.34	0.89	2.48	1.00	7.04	1.33	3.11	0.95	0.55	0.97	14
1.24	2.09	3.05	0.22	3.02	6.12	0.75	0.26	2.22	0.96	4.29	15

Table 6. Absolute error in space-time for 14^{th} iteration of Case 4

(t,x)	-3.0	-2.0	-1.0	1.0	2.0	3.0
0.1	7.01×10^{-8}	5.45×10^{-8}	4.11×10^{-8}	4.16×10^{-8}	5.74×10^{-8}	7.33×10^{-8}
0.3	2.01×10^{-7}	6.32×10^{-8}	5.04×10^{-8}	5.92×10^{-8}	6.14×10^{-8}	1.88×10^{-7}
0.5	1.02×10^{-6}	1.62×10^{-7}	2.92×10^{-8}	2.00×10^{-8}	2.22×10^{-7}	1.10×10^{-6}

Table 7. Absolute error in space-time for 14^{th} iteration of Case 5

(t,x)	-3.0	-2.0	-1.0	1.0	2.0	3.0
0.1	6.21×10^{-8}	5.85×10^{-8}	1.21×10^{-8}	1.16×10^{-8}	5.24×10^{-8}	6.04×10^{-8}
0.3	4.71×10^{-7}	4.82×10^{-8}	2.03×10^{-8}	1.92×10^{-8}	4.54×10^{-8}	3.21×10^{-7}
0.5	8.58×10^{-7}	5.72×10^{-7}	6.02×10^{-8}	6.60×10^{-8}	5.02×10^{-7}	8.01×10^{-7}

Table 8. Absolute error in space-time for 15^{th} iteration of Case 6

(t,x)	-3.0	-2.0	-1.0	1.0	2.0	3.0
0.1	8.33×10^{-8}	7.01×10^{-8}	6.22×10^{-9}	6.29×10^{-9}	6.98×10^{-8}	8.17×10^{-8}
0.3	2.21×10^{-8}	3.08×10^{-8}	7.22×10^{-9}	6.96×10^{-9}	2.98×10^{-8}	4.74×10^{-8}
0.5	6.37×10^{-7}	4.91×10^{-7}	3.08×10^{-8}	2.31×10^{-8}	5.05×10^{-7}	5.68×10^{-7}

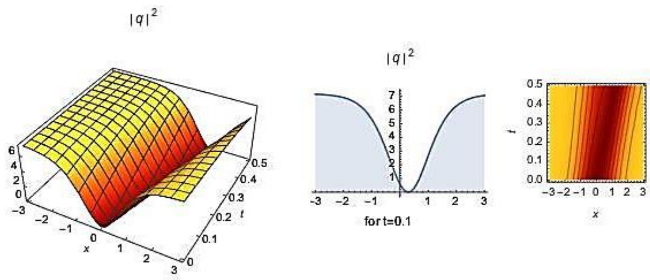

Fig. 4. 3D, 2D and density graphics for Case 4 (color online)

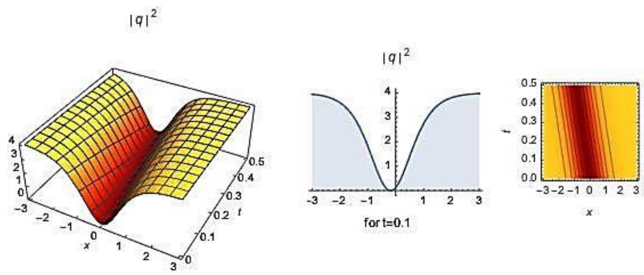

Fig. 5. 3D, 2D and density graphics for Case 5 (color online)

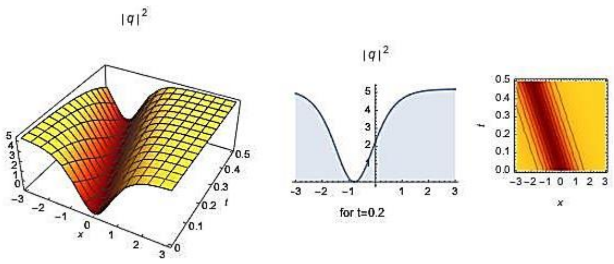

Fig. 6. 3D, 2D and density graphics for Case 6 (color online)

5. Conclusions

This paper numerically studied bright and dark CQ solitons to the LPD model by the adopted LADM scheme. Bright and dark soliton solutions are studied, and the surface plots are presented. The error tables also point to the fact that this adopted algorithm is a powerful scheme that can be successfully applied to handle soliton solutions in birefringent fibers. This is therefore going to be the next venture with the current model and its results are currently awaited and are surely going to be visible soon.

References

[1] J. Vega-Guzman, A. Biswas, A. H. Kara, M. F. Mahmood, M. Ekici, H. M. Alshehri, M. R. Belic, J. Nonlinear Opt. Phys. Mater. **30**, 2150007 (2021).

[2] Y. Yildirim, E. Topkara, A. Biswas, H. Triki, M. Ekici, P. Guggilla, S. Khan, M. R. Belic, J. Opt. **50**, 322 (2021).

[3] A. Biswas, J. Edoki, P. Guggilla, S. Khan, A. K. Alzahrani, M. R. Belic, Ukr. J. Phys. Opt. **22**, 123 (2021).

[4] O. González-Gaxiola, A. Biswas, H. M. Alshehri, M. R. Belic, J. Comp. Electronics. **20**(3) 1216 (2021).

[5] O. González-Gaxiola, A. Biswas, Q. Zhou, H. M. Alshehri, J. Nonlinear Opt. Phys. Mater. **31**(3), 2250009 (2022).

[6] O. González-Gaxiola, A. Biswas, M. Ekici, S. Khan, J. Opt. **51**(1), 29 (2022).

[7] O. González-Gaxiola, A. Biswas, A. K. Alzahrani, Open Phys. **18**, 182 (2020).

[8] O. González-Gaxiola, A. Biswas, A. K. Alzahrani, M. R. Belic, J. Comput. Electron. **20**, 1216 (2021).

[9] G. Adomian, R. Rach, J. Math. Anal. Appl. **114**, 171 (1986).

[10] G. Adomian, Kluwer, Boston (1994).

[11] J.-S. Duan, Appl. Math. Comput. **217**, 6337 (2011).

[12] M. M. Hosseini, H. Nasabzadeh, Appl. Math. Comput. **182**, 536 (2006).

[13] E. Babolian, J. Biazar, Appl. Math. Comput. **130**, 383 (2002).

*Corresponding author: biswas.anjan@gmail.com